Applied Catalysis B: Environmental 168-169 (2015) 342–352

Contents lists available at ScienceDirect

Applied Catalysis B: Environmental

journal homepage: www.elsevier.com/locate/apcatb

Stability and activity of Pd-, Pt- and Pd–Pt catalysts supported on alumina for NO oxidation

Xavier Auvray, Louise Olsson*

Chemical Engineering, Competence Center for Catalysis, Chalmers University of Technology, S-412 96 Göteborg, Sweden

ARTICLE INFO

Article history:
Received 11 September 2014
Received in revised form
18 December 2014
Accepted 21 December 2014
Available online 14 January 2015

Keywords:
NO oxidation
Diesel oxidation catalyst
C_3H_6 inhibition
Pt–Pd
DRIFT
TPR

ABSTRACT

The association of palladium and platinum supported on alumina was studied for diesel oxidation catalyst application. The effect of propene, water and their combination on NO oxidation activity was investigated in flow reactor over Pt/Al_2O_3, Pd/Al_2O_3 and two $Pt–Pd/Al_2O_3$ catalysts, prepared by co-impregnation and sequential impregnation of the metals. Contrary to Pd/Al_2O_3, activity improvement due to the repetition of activity test was observed on Pt/Al_2O_3 and both $Pt–Pd/Al_2O_3$. Metal sintering during activity test was revealed by CO chemisorption. The bimetallic catalysts reached their final stability and activity before Pt/Al_2O_3. The presence of water decreased the NO oxidation activity of all catalysts and the propene completely inhibited NO oxidation at low temperature until propene combustion occurred. The addition of palladium to Pt/Al_2O_3 was found very efficient to oxidize propene and therefore significantly limited the inhibition of NO oxidation by propene. A mechanism was proposed to explain the NO oxidation promotion lying behind the addition of Pd. DRIFT measurements and flow reactor experiments showed that propene was less stable and able to react with surface nitrates on Pd-containing catalyst at low temperature (175 °C). On Pt/Al_2O_3, however, the propene consumption proceeded initially through selective catalytic reduction of NO, which took place at higher temperature (240 °C). In this way, propene combustion and consequently NO oxidation occurred at lower temperature on bimetallic catalysts than on Pt/Al_2O_3.

1. Introduction

In diesel exhaust after treatment, the catalyst is exposed to a complex gas mixture, the composition of which varies with the engine load, and is sometimes subjected to high temperature. Under these harsh conditions, sintering of Pt/Al_2O_3 oxidation catalysts has been observed and attributed to both thermal and chemical effects [1–4]. The addition of palladium in the DOC formulation has led to higher resistance against metal particle sintering [5–9], without altering the NO oxidation [6,10] despite the low activity of Pd-catalysts for this reaction. Another issue is the presence in the exhausts of various compounds that can interfere with the considered reaction by, for instance, competing for the catalytic active sites. Among these DOC poisons, residual SO_2 has been widely studied [11–16] but mutual inhibition of reactants to be oxidized has also raised interest. CO and NO have been found to affect each others' oxidation [17–19] as well as CO and C_3H_6 [20]. The presence of hydrocarbons decreases NO oxidation activity of Pt/Al_2O_3 and vice versa [21–23]. However, inhibition of NO oxidation by hydrocarbons has only been investigated on Pt/Al_2O_3, which needs to be extended to catalysts with different active phase in order to increase the knowledge about inhibition mechanism and to develop a catalyst formulation capable of limiting this inhibition.

In this work the effect of water and propene on Pt/Al_2O_3, Pd/Al_2O_3 and bimetallic $Pt–Pd/Al_2O_3$ DOCs was investigated using NO oxidation as probe reaction. The stability of the catalysts in operating conditions was also addressed and DRIFT spectroscopy was used to get a deeper understanding about the reaction mechanisms. In addition, H_2 TPR were performed before and after NO oxidation experiments in order to examine the reproducibility of different oxygen species on the surface.

2. Experimental

2.1. Catalysts preparation

2.1.1. Pt/Al_2O_3 and Pd/Al_2O_3

Two monometallic catalysts containing 1 wt% Pt and 1 wt% Pd respectively have been prepared according to the same procedure. A slurry consisting of pre-calcined γ-alumina (Puralox SBa-200, Sasol, 2.5 h at 750 °C) and purified deionized "MilliQ" water (Millipore) was maintained under stirring while the pH was monitored.

* Corresponding author. Tel.: +46 31 772 4390; fax: +46 31 772 3035.
E-mail address: louise.olsson@chalmers.se (L. Olsson).

http://dx.doi.org/10.1016/j.apcatb.2014.12.035
0926-3373/

A ratio of 16 mL water per gram of alumina was used. Nitric acid was then added drop-wise to reach a stable pH of ca. 4. A solution containing the PGM was prepared by dilution of the appropriate amount of metal precursor, $Pt(NO_3)_2$ and $Pd(NO_3)_2$, respectively, in 40 mL MilliQ water. It was then added drop-wise to the stirred alumina slurry. During this operation, the pH decreased. After ca. 2 h under stirring, the solution was frozen by using liquid N_2 and dried overnight under vacuum to sublimate the water. The collected catalyst powder was calcined at 500 °C for 2 h.

2.1.2. Pt–Pd/Al_2O_3 by co-impregnation of Pt and Pd

One bimetallic catalyst containing both platinum and palladium was prepared by wet impregnation, freezing and drying, as described for the monometallic catalysts. However, the solution added to the alumina slurry contained both $Pt(NO_3)_2$ and $Pd(NO_3)_2$, in such proportion to obtained a total PGM loading of 1 wt% with a Pt/Pd mass ratio of 3. This catalyst was referred to as PtPd-CoImp in the present manuscript.

2.1.3. Pt–Pd/Al_2O_3 by sequential impregnation of Pt and Pd

A second bimetallic catalyst containing Pt and Pd in the same proportion as PtPd-CoImp (1 wt% PGM, Pt/Pd = 3) was prepared by sequential impregnation. First 0.75 wt% Pt/Al_2O_3 was prepared as described above in the case of monometallic Pt/Al_2O_3. After calcination at 500 °C, the catalyst powder was mixed with MilliQ water in the proportion 16 mL/g cat and the pH was decreased by addition of HNO_3 to ca. 4. A 10 mL solution containing the palladium precursor was prepared and added drop-wise. The catalyst was then frozen, dried and calcined for two hours at 500 °C. This catalyst was named PtPd-Seq.

2.1.4. Monolith preparation

The four catalysts studied were washcoated onto honeycomb-structured cordierite monoliths by dipping a pre-calcined (2 h at 600 °C in air) monolith in a catalyst powder suspension. The monoliths were 2 cm long and had a 2 cm diameter and a channel density of 400 cpsi. The catalyst powder was mixed with a binder (boehmite Disperal P2, Sasol, 80 wt% catalyst/20 wt% binder) and dispersed in a solution made of 50 wt% ethanol and 50 wt% water. The liquid-to-solid mass ratio of the slurry was around 7 to ensure the deposition of a sufficient amount of washcoat and avoid channel clogging. After each dipping, the monolithic sample was dried with a hot air gun at ca. 90 °C until the liquid phase in the channels disappear. Drying at 550 °C was then performed for one minute. During the first drying step, the sample was continuously rotated with care to ensure the homogeneous wetting of the channels. The dipping and drying process was repeated until ca. 0.5 g washcoat was deposited. The monoliths were then calcined in oven at 550 °C in air for two hours.

2.1.5. Flow reactor experiments

A flow reactor was used to measure the activity and selectivity of the samples. It consists of a horizontal quartz tube in which the monolith was placed and the gas mixture, supplied by Bronkhorst® mass flow controllers, flowed. The reactor was heated by a resistance connected to a Eurotherm temperature controller. Quartz wool was wrapped around the reactor to provide thermal insulation. A MultiGas™ 2030 FTIR continuous gas analyzer (MKS) was connected to the reactor outlet and monitored the concentrations of the various gas constituents.

Initially, the samples were exposed to a degreening treatment in the flow reactor, consisting of 2 h at 500 °C using 500 ppm NO, 8% O_2 in Ar and a total flow of 3000 mL/min. Thereafter, the dispersion was measured using CO-chemisorption, the details of which are described in the following section. After, the dispersion measurement the catalysts were subjected to repeated thermal cycles under a gas flow of 3000 mL/min containing 500 ppm NO, 8% O_2 and argon as carrier gas. The temperature was increased and then decreased at a controlled rate of 5 °C/min from 150 °C to 500 °C, describing one cycle. Four cycles, were performed in one run. In the second cycle, 5% H_2O was included in the gas mixture previously described so as to study the effect of water. In the third cycle, the combined effect of water and propene on NO oxidation was addressed; therefore 500 ppm C_3H_6 was added to the second cycle gas mixture. Finally water was turned off during the fourth cycle in order to study the effect of propene in dry conditions. This procedure was designed in order to study the effect of water, C_3H_6 – a model hydrocarbon – and the combination of water and propene on the NO oxidation activity of the Pt, Pd and bimetallic Pt–Pd catalysts. Before each cycle the catalyst was pre-treated with 10% O_2 in Ar at 450 °C for 10 min followed by 30 min reduction at 450 °C in 2% H_2, with a total flow of 1000 mL/min.

The cycle run described above was repeated three times in order to assess the reproducibility of the results, as well as the aging and stability of each catalyst.

2.2. Catalyst characterization

2.2.1. BET and CO chemisorption

Chemisorption of CO was used to assess the metal dispersion of mono-metallic catalysts since the amount of surface metal atoms can be correlated to the amount of CO chemisorbed. After reduction of the catalyst at 450 °C in a H_2 flow (2% in Ar) for 30 min, the reactor was cooled rapidly to 25 °C. After flushing with argon for 10 min, 100 ppm CO in Ar was flowed for 20 min to measure the CO adsorption. Physisorbed CO was then flushed with Ar for 500 s and a second 100 ppm CO pulse (10 min) was carried out to quantify the weakly bonded CO. During these measurements a total flow of 1000 ml/min was used.

However, the dispersion of bimetallic Pt–Pd catalysts cannot be inferred from CO chemisorption without important assumptions since the adsorption stoichiometry of CO on Pt and Pd is different. Attempt of calculating the dispersion, in the bimetallic cases, would require detailed information about the presence of alloy particles, their composition and, more importantly, the exact composition of their surface. For these reasons, the results of CO chemisorption were merely reported as the ratio CO_{ads}/M, M being the amount of noble metal, in mol.

The surface area was determined by physisorption of nitrogen at liquid nitrogen temperature and calculated according to the BET method. After degassing the powder samples at 250 °C for 2 h under vacuum, the measurement was performed on a Micromeritics TriStar 3000 chemisorption instrument.

2.2.2. Temperature-programed reduction (TPR)

TPR was performed to characterize the reducibility of the catalysts after exposure to oxygen-rich gas flow. About 0.05 g of catalyst powder (0.1 g in the case of Pt/Al_2O_3 catalyst) was loaded in a vertical tubular quartz reactor (inner diameter = 5 mm) on a sintered quartz bed. A controlled gas mixture flowed downward through the catalyst bed while a mass spectrometer (Hiden Analytical) enabled to measure the time-resolved hydrogen concentration of the outlet gas flow. Prior to the TPR, the catalysts were degreened for 2 h at 500 °C under a flow containing 500 ppm NO and 8% O_2 with Ar as inert balance. After this treatment, the catalysts were reduced at 450 °C for 30 min in 2% H_2. Then, the catalysts were exposed to O_2 (8% balanced with Ar) at 450 °C for 30 min and during subsequent cooling to 25 °C (10 °C/min). After a one-hour argon flush, the pre-oxidized catalysts were exposed to 500 ppm hydrogen (balanced with Ar) for 30 min at 25 °C and during a subsequent temperature ramping step to 450 °C (10 °C/min). The catalysts were then aged for 2 h at 500 °C (500 ppm NO and 8% O_2 with Ar as inert balance) to mimic the effect of one NO oxidation activity measurement. The

Table 1
Catalytic surface characterization: BET surface area and CO chemisorption measurements.

Catalyst	CO/PGM (mol%)		BET surface area
	Degreened	After 3rd run	(m^2/g)
Pt/Al_2O_3	15.6	2.3	158
Pd/Al_2O_3	6.2	4.9	165
PtPd-Seq	38.8	11.9	159
PtPd-CoImp	23.7	6.4	165

TPR procedure was then repeated to evaluate the effect of NO oxidation step on the catalysts reducibility. The total flow through the whole experiment was kept constant at 20 mL/min.

2.2.3. DRIFT spectroscopy

In situ DRIFT experiments were conducted with a BioRad FTS 6000 spectrometer equipped with a heated reaction cell with KBr windows (Harrick Scientific, Praying Mantis), in which the catalyst powder was placed. The temperature was regulated by a Eurotherm 2416 controller. Mass flow controllers (Bronkhorst Hi-Tech) were used to supply the gases to the reaction cell. The catalysts were pretreated at 500 °C for 2 h with a gas flow containing 500 ppm NO and 8% O_2 in Ar. The total flow used was 100 mL/min in every experiment. Before NO and/or C_3H_6 adsorption, oxidation with 8% O_2 in Ar (10 min at 450 °C) followed by reduction with 2% H_2 in Ar (30 min at 450 °C) was performed. Adsorption of 1000 ppm NO + 8% O_2 was performed for 30 min at 150 and 250 °C. The same exposure was repeated with additional 1000 ppm C_3H_6.

3. Results and discussion

3.1. Catalyst characterization

The results of the BET surface area measurements on the fresh samples, reported in Table 1, indicate that all catalysts had similar surface area, around 160 m^2/g. However, a significantly larger CO adsorption was noted on PtPd-Seq, prepared by sequential impregnation, than on PtPd-CoImp, which indicates a higher metal dispersion in the case of sequential impregnation. The results of CO adsorption (Table 1) also show that the dispersion of all four catalysts decreased due to the repetition of the activity tests. The larger adsorption of CO measured on fresh PtPd-Seq persisted after the series of experiments.

The results of the TPR before and after the NO oxidation aging step are shown in Fig. 1. Note that about 100 mg sample is used for Pt/Al_2O_3, while 50 mg for the other samples. Large differences in reducibility and behavior upon aging appeared between Pt/Al_2O_3 (Fig. 1a) and Pd/Al_2O_3 (Fig. 1b). Negligible H_2 uptake was measured at 25 °C for the platinum sample while H_2 was exclusively consumed at 25 °C by the palladium catalyst. This indicates the facile reduction of palladium oxide. Hydrogen uptake by Pt/Al_2O_3 occurred mainly in the temperature ramping between 40 °C and 280 °C. The amounts of consumed H_2 reported in Table 2 indicate a larger uptake on the Pd catalyst due to the larger molar amount of Pd. Formation of Pd hydride may have contributed to the hydrogen consumption. After aging at 500 °C in NO oxidation conditions, the H_2 uptake profile of Pd/Al_2O_3 remained unchanged. In contrary, H_2 consumption of the aged Pt/Al_2O_3 was larger and occurred between 40 °C and 450 °C, reflecting the larger extent of platinum oxidation and the higher stability of the oxide formed after the aging step. Like Pt/Al_2O_3, the two Pt–Pd/Al_2O_3 samples exhibited negligible uptake at 25 °C (Fig. 1c and d), which indicates the presence of no or very few isolated Pd particles. The H_2 consumption was larger for PtPd-CoImp and possessed the maximum peak at significantly higher temperature (around 125 °C) than for PtPd-Seq (around 95 °C). After the NO oxidation step at 500 °C, the amount of H_2 consumed by PtPd-Seq (Fig. 1c) was similar as before. However, like for Pt/Al_2O_3, a second reduction peak developed at high temperature (maximum at ≈320 °C) while the low temperature peak decreased and shifted toward higher temperature (maximum at ≈120 °C). For PtPd-CoImp the aging step yielded lower H_2 consumption and a slight shift of the reduction peak toward higher temperature. The reason for the lower hydrogen consumption could be sintering of the noble metal. PtPd-Seq unlike PtPd-CoImp was able to form strong oxide species. However, based on the reduction temperature, this oxide was less strong than the oxide observed on aged Pt/Al_2O_3. The addition of Pd to Pt/Al_2O_3 increased the H_2 consumption of the degreened sample, which can be attributed to the higher metal molar content (identical weight content 1 wt%) and the high capacity of Pd to adsorb hydrogen. However, for aged catalysts, alloying Pt with Pd lowered the temperature of reduction as well as the H_2 consumption. Addition of Pd to Pt/Al_2O_3 for NO oxidation application improved the resistance to platinum oxide formation. This effect was more pronounced on the sample prepared by co-impregnation, which did not develop the high temperature reduction peak after aging, typical of Pt/Al_2O_3.

Table 2
Hydrogen consumed during TPR (integration of TPR profiles from $t = 0$) before and after the aging step.

	H_2 consumed (μmol/g_{cat})	
	Before aging	After aging
Pt	22	32
Pd	93	87
PtPd-Seq	43	43
PtPd-CoImp	59	41

3.2. Improvement induced by the repetition of activity test

The activity test procedure, composed of four thermal cycles separated by oxidation and reduction steps, was carried out three times to evaluate the reproducibility of the results and the modification of the catalyst in operating conditions. The results are reported in Fig. 2 as the conversion of NO into NO_2 measured during the four temperature-programmed cycles conducted in different gas mixtures. The catalytic oxidation of NO over Pt/Al_2O_3 is kinetically limited at low temperature and restricted by the thermodynamic equilibrium at high temperature. Hence, one conversion maximum was obtained when the temperature was ramped up and a second maximum was obtained during the controlled cooling. The conversion profiles obtained during the three runs performed on each sample are represented in order to evaluate the activity changes occurring in operating conditions. Fig. 2a shows that the catalytic activity of Pt/Al_2O_3 was improved by the repetition of cycles. It depicts a structural change of the catalyst during the experimental procedure, which was confirmed by the lower amount of chemisorbed CO measured after the repetition of cycles (Table 1) and the TPR profiles (Fig. 1a). A marked improvement was observed in the second run compared to the first one, while a moderate activity increase was noted between the second and third run. Pt/Al_2O_3 catalysts are known to be more active for NO oxidation after Pt sintering and formation of larger platinum particles [1,18,24–27]. The shape of the particles as well as the aging conditions also affects the catalytic activity [1,2,12]. The slow activity improvement of Pt/Al_2O_3 can be correlated to the structural transformation that led to the development of strong Pt oxide revealed by the TPR (Fig. 1a). In contrary, Pd/Al_2O_3 seemed to be insensitive to the repetition of cycles, as shown in Fig. 2b. This catalyst presented two activity peaks during the heating and only one, the most intense, during cooling. Compared to Pt/Al_2O_3, Pd/Al_2O_3 exhibited low activity for NO oxidation but stable behavior, showed

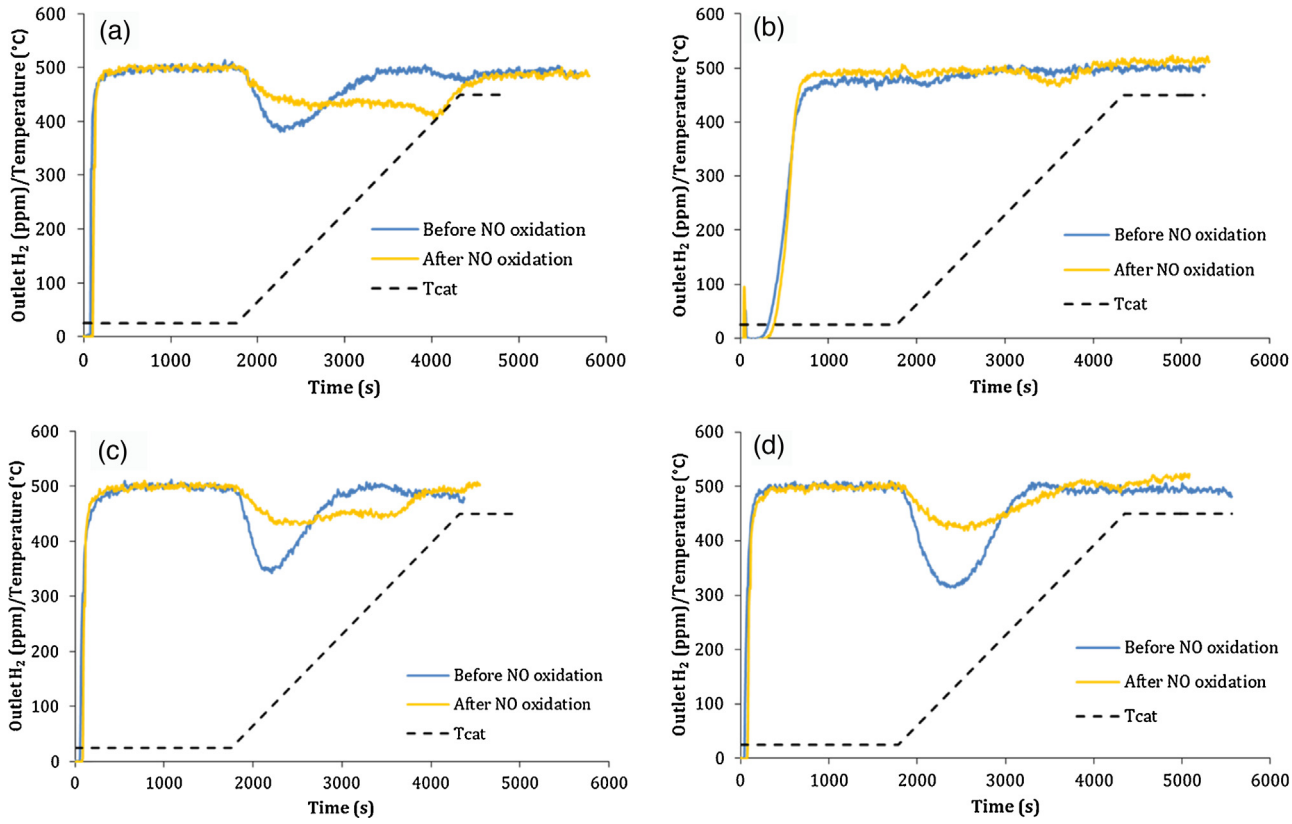

Fig. 1. Temperature-Programed Reduction (TPR) profiles (500 ppm H_2 starting at $t = 0$) before and after aging in NO oxidation conditions (500 ppm NO + 8% O_2 in Ar, 2 h at 500 °C). (a) Pt/Al_2O_3, (b) Pd/Al_2O_3, (c) PtPd-Seq and (d) PtPd-CoImp. 100 mg sample is used for Pt/Al_2O_3, and 50 mg for the other samples.

by the similar activity measured in all three runs. The stability of Pd/Al_2O_3 was also observed by the chemisorption of CO showing a relatively small evolution after the activity cycles. The nearly identical H_2 profiles obtained by TPR measurements before and after NO oxidation (Fig. 1b) confirmed the stability of Pd/Al_2O_3. Repetition of activity tests, oxidation and reduction periods did not affect the activity of Pd/Al_2O_3.

The bimetallic catalysts, regardless the preparation method, displayed very close activity during the second and the third run (Fig. 2c and d), indicating the early occurrence of the catalyst structure changes, namely during the first run of the activity test protocol. The bimetallic catalyst prepared by simultaneous impregnation of Pd and Pt into the alumina support (PtPd-CoImp) reached its final activity and surface structure already after the third cycle, in presence of propene and water, of the first run since it can be seen in Fig. 2d that similar NO conversion was measured in all three runs in presence of propene (4th cycle). This catalyst showed, therefore, a faster stabilization than the bimetallic catalyst prepared by stepwise impregnation of Pt and Pd, with Pt deposited first on the alumina (PtPd-Seq). Indeed, following the same interpretation, it can be seen in Fig. 2c (PtPd-Seq) that the NO conversion during the fourth cycle of the first run was generally lower than the one reported for the third run, indicating an incomplete stabilization process at that stage. This difference can be ascribed to the preparation method. The TPR results support the faster stabilization of PtPd-CoImp since the reduction of H_2 consumption was the main effect of NO oxidation while PtPd-Seq developed a second high temperature reduction peak, which was identified as a possible cause of the slow stabilization of Pt/Al_2O_3.

In general, the bi-metallic Pt–Pd catalysts evolved faster and reached durable activity at earlier stage than the mono-metallic Pt/Al_2O_3. Many studies have shown that the addition of palladium into Pt/Al_2O_3 catalysts limited platinum sintering and increased the thermal stability of metallic particles by the formation of Pt–Pd alloy [5,6,9,10], which can explain our findings.

3.3. Conditions favoring catalyst transformation

We further examined the main factors responsible for the transformation. The catalytic activity evolution with time and gas flow composition can be observed in Fig. 2. In a given gas composition, a large increase of activity would indicate a rapid transformation induced by the gas mixture. Conversely, a regular activity increase, run after run, without any dramatic increase from one cycle to the next would be the sign of stabilization by thermal treatment and/or oxidation and reduction cycles. In this analysis, the activity increase was related to the final stable activity. Fig. 2a shows that for Pt/Al_2O_3, the activity difference between two consecutive runs was similar in each of the four cycles, indicating a continuous transformation, which was influenced by the thermal treatment and the oxidation-reduction steps in the pre-treatment rather than the reactive atmosphere of the activity test.

The two $Pt–Pd/Al_2O_3$ catalysts showed a different evolution. It can be seen in Fig. 2 c and d that during the first run, the activity gap, related to the second and third run, was closing up. In particular, during the second cycle, in presence of 5% water, the conversion was much higher and closer to the third run profile during cooling (second peak) than during heating (first peak). This indicates a change in the catalyst active phase attributable to the presence of water, which caused an improvement in NO oxidation activity. This observation applied to both catalysts and can be made for the third cycle, carried out in combined presence of 5% water and 500 ppm propene, although it was less pronounced due to the already good stability of the samples.

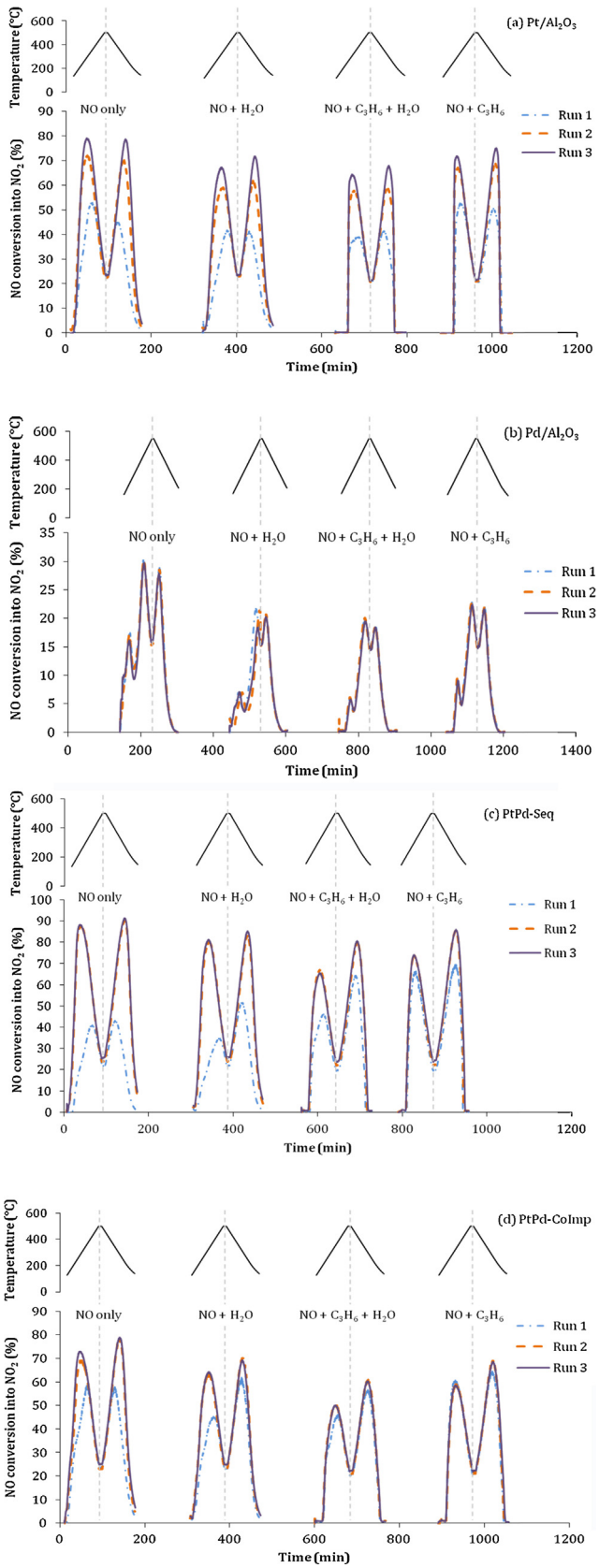

Fig. 2. The conversion of NO during one full cycle (500 ppm NO + 8% O_2 in absence and presence of 5% H_2O and/or 500 ppmC_3H_6) is represented for each catalyst. (a) Pt/Al_2O_3 (b) Pd/Al_2O_3 (c) $Pt–Pd/Al_2O_3$ prepared by sequential impregnation and (d) $Pt–Pd/Al_2O_3$ prepared by co-impregnation. The results of the three repeated runs are reported.

Based on the activity results from repeated experiments and CO chemisorption, it was clear that the catalysts were subjected to structural changes, even after a degreening step, leading to an improvement in activity. Tao et al. [28] have studied the restructuring of bimetallic catalysts with gas environment. They determined the structure of Pt–Pd particles composed of a platinum core and a palladium shell in as-prepared catalysts. This structure is in agreement with other studies [29–31]. However, Tao et al. [28] did not observed structural changes upon exposition of Pt-Pd catalysts to oxidizing and reducing conditions, with palladium remaining at the alloy particle surface. Transformation of Pd to PdO was, however, noted. Morlang et al. [8] have observed the enrichment of particle surface with Pd and the formation of PdO on the support and on the Pt particles upon hydrothermal aging. The modifications and stabilization occurred at different stage depending on the catalysts, as seen in Fig. 1. Thus, it was noticed that the bimetallic catalysts, regardless of the impregnation method, reached stability earlier than Pt/Al_2O_3 while Pd/Al_2O_3 was not affected by the repetition of activity tests runs. The experimental data suggest that water accelerated the stabilization process of the $Pt–Pd/Al_2O_3$ catalysts, while no obvious chemical effect was detected in the case of Pt/Al_2O_3. The following results reported in this study were obtained from the third run, after the catalyst had been stabilized.

3.4. NO oxidation activity

In Fig. 3, the activity of all catalysts was compared for NO oxidation in dry conditions when the temperature was increased and then decreased with 5 °C/min for Run 3. It confirmed the lower activity of the Pd/Al_2O_3 catalyst in both phases. The most efficient catalyst was PtPd-Seq which was able to reach 91% conversion at 250 °C during cooling. Pt/Al_2O_3 and PtPd-CoImp showed similar activity profile during cooling, while Pt/Al_2O_3 was slightly more active during heating. The correlation of the activity results with the TPR results of aged catalysts presented in Fig. 1 suggests that the ability to form strong oxide as aged Pt/Al_2O_3 and PtPd-Seq do is beneficial for NO oxidation. However the stability of the formed platinum oxide should not be too high to obtain the best NO conversion. It is worth to note that during cooling, PtPd-Seq and PtPd-CoImp showed a better activity than during heating while the monometallic catalysts showed a slight deactivation during cooling. Pt/Al_2O_3 was less active at low temperature during cooling although the top conversion was the same in both phases. It is known that, at low temperature, platinum oxide can form due to the high oxygen concentration and the formation of NO_2 [17,19,25,26,32] and that platinum oxide is less active for NO oxidation than metallic Pt. During cooling, Pd/Al_2O_3 presented lower activity in general and the low temperature peak disappeared. This peak, present in heating and absent in cooling, might be related to the reducing treatment carried out before every activity cycle since the catalyst was reduced at the start of the heating ramp and became oxidized during experiment. It should be mentioned that the bi-metallic samples contain more noble metals on a molar base compared to the Pt sample ($6.2 \cdot 10^{-5}$ mol/g for $Pt/Pd/Al_2O_3$ and $5.1 \cdot 10^{-5}$ mol/g for Pt/Al_2O_3). However, Pd shows a very low NO oxidation activity (Fig. 3), for example the conversion for the cooling ramp (Fig. 3b) at 300 °C and below was less than 2%, thus the increased activity seen for PtPd-Seq was not due to the higher molar amount of noble metal, but instead likely connected to the interactions between Pt and Pd.

3.4.1. Effect of water and propene on NO oxidation activity

In this section, the effect of the presence of water and propene in the inlet gas on the oxidation of NO was addressed. The temperature-programmed activity test was repeated in various conditions involving these constituents. The conversion obtained

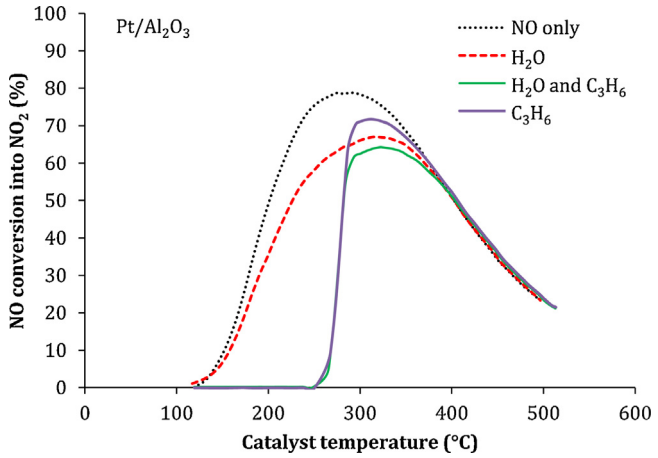

Fig. 4. NO conversion profiles obtained, during heating (5 °C/min), with Pt/Al_2O_3 in various gas conditions: 500 ppm NO, 8% O_2 in Ar only and with 5% H_2O and/or 500 ppm C_3H_6.

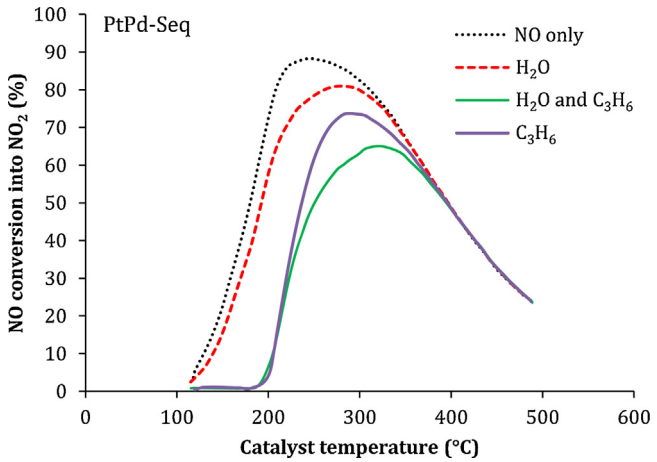

Fig. 5. NO conversion profiles obtained, during heating (5 °C/min), with $Pt–Pd/Al_2O_3$, prepared by sequential impregnation, in various gas conditions: 500 ppm NO, 8% O_2 in Ar only and with 5% H_2O and/or 500 ppm C_3H_6.

during the third series, when the catalysts had already been stabilized, in the different cases is compared.

In Fig. 4, it can be seen that the best performance was obtained in dry conditions, i.e. in absence of both water and propene over Pt/Al_2O_3 catalyst, with a maximum conversion of 79%. The addition of water in the reaction gas mixture inhibited the NO oxidation, illustrated by the lower maximum conversion attained (67%). The negative effect of water has been investigated [19,21] on Pt/Al_2O_3 catalysts and was attributed to the competitive adsorption of water on the NO adsorption sites by Olsson et al. [21]. The presence of propene decreased also the maximum conversion attained compared to dry conditions but its main effect was to increase tremendously the light-off temperature of the catalysts. On Pt/Al_2O_3, the total suppression of activity was observed in presence of propene, independently of the water presence, until a specific temperature. This temperature corresponds to the light-off temperature of propene combustion indicating the occupation of NO oxidation active sites by propene. Thus, the oxidation of NO could only take place when the combustion of propene freed the active sites. The consumption of NO_2 in the C_3H_6 oxidation reaction was also invoked in literature [22,23,33] to explain the NO oxidation inhibition by propene. Al-Harbi et al. [23] reported the low temperature oxidation of propene by NO_2. At high temperature, propene was converted to water and carbon dioxide, which could, in turn, inhibit NO oxidation and explain the lower activity compared to NO only. The lowest activity for the Pt/Al_2O_3 sample was received in the simultaneous presence of water and propene. The reason is the overall lower conversion due to water and a high light-off temperature specific to the propene inhibition effect. It should be noted that after the reaction ignition, better activity was obtained in presence of propene than in presence of water. Fig. 4 presents only the results acquired during the heating phase but the same characteristics and effects of water and propene were observed during the cooling phase.

The results obtained on the bimetallic PtPd-Seq are reported in Fig. 5. The effect of water is similar to the one described above for Pt/Al_2O_3. Namely, the NO conversion into NO_2 was lowered in presence of water. The presence of propene also inhibited the oxidation of NO as displayed in Fig. 5. However, even at temperatures higher than the propene combustion light-off, propene had a more pronounced detrimental effect than water. This result differs from the observation made in the case of Pt/Al_2O_3 sample. The inhibition of water and C_3H_6 was, however, additive like on Pt/Al_2O_3. Consequently, the lowest activity was noted in simultaneous presence of water and propene.

Fig. 6 displays the activity profiles in various conditions of the second bimetallic catalyst, PtPd-CoImp. Similar effects of water and propene as on PtPd-Seq can be noted. The highest activity was measured in absence of both water and propene, while the lowest performance was observed in presence of these two components in the gas feed. As for PtPd-Seq the detrimental effect of propene was more pronounced than the water one.

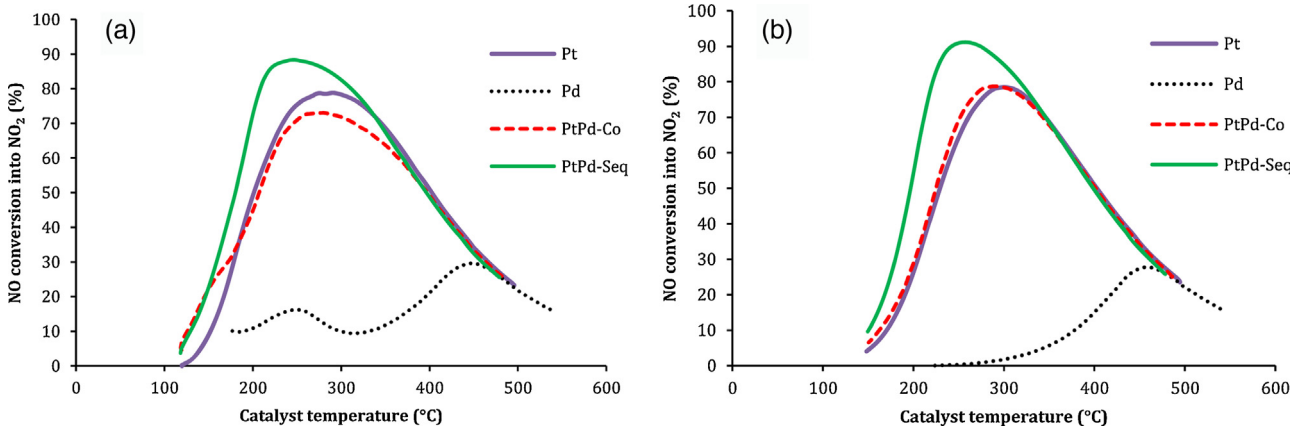

Fig. 3. Comparison of the catalysts ability to convert NO into NO_2 during a temperature-programmed experiment in a gas flow containing only 500 ppm NO, 8% O_2 and Ar. (a) Conversion during the heating phase (5 °C/min) and (b) cooling phase (−5 °C/min).

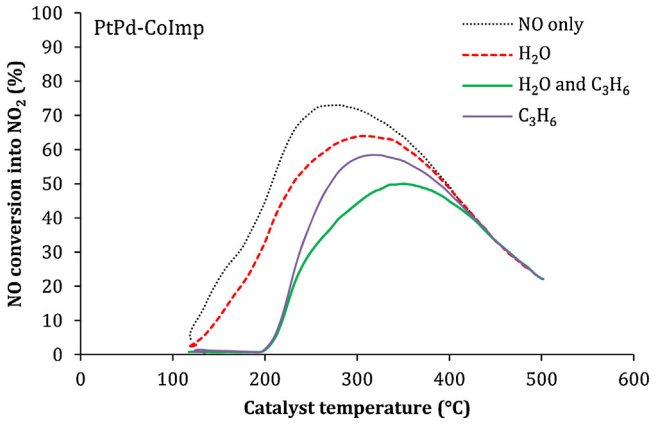

Fig. 6. NO conversion profiles obtained, during heating (5 °C/min), with Pt–Pd/Al_2O_3, prepared by co-impregnation, in various gas conditions: 500 ppm NO, 8% O_2 in Ar only and with 5% H_2O and/or 500 ppm C_3H_6.

The combined effect of water and propene led to a significant loss of activity on all the three catalysts discussed above. It can also be noted that the NO oxidation breakthrough in presence of propene took place at the same temperature with and without 5% water, which means that until this characteristic temperature, the inhibition was driven by the presence of propene. When water and propene were present, the effect of water was limited until combustion of propene and was expressed at higher temperature.

3.4.2. Propene inhibition and oxidation

There are clear differences in the effect of propene between the catalysts and therefore the NO conversion profiles of the four catalysts in presence of propene are presented in Fig. 7. The catalyst showing the highest maximum conversion was PtPd-Seq followed by the Pt catalyst and the PtPd-CoImp. (Note that the maximum conversion occurs at different temperatures for different catalysts). The Pd catalyst exhibited very low NO conversion. On bimetallic catalysts, NO oxidation started at significantly lower temperature (ca. 180 °C) than on Pt/Al_2O_3 and Pd/Al_2O_3 catalysts (ca. 250 °C). This was explained by the much lower light-off temperature of the oxidation of propene on bimetallic catalysts. Indeed, in absence of water, the temperature at which 50% of the propene had been converted was >240 °C for the Pt catalyst but only ≈175 °C for the bimetallic catalysts (Table 3). It is worth to note that, for propene oxidation, the Pd catalyst showed lower T_{50} (>200 °C) than Pt catalyst despite its poor activity for NO oxidation. Interestingly, the Pd only catalyst contains more palladium compared to the bi-metallic catalysts but the T_{50} was still higher for the Pd catalyst. The addition of platinum to palladium-based catalysts is therefore a great advantage for the combustion of propene, decreasing significantly the light-off temperature of the mono-metallic catalysts. One possible reason could be that NO is inhibiting the propene oxidation and the addition of platinum results in an increased NO oxidation, which decreases the inhibition. Additionally, there might be NO_2 formed that reacts with propene in an SCR mechanism. Further, the bimetallic catalysts are more active for NO oxidation since the palladium in the bimetallic catalyst increases the activity for propene oxidation and thereby limit the inhibiting effect of propene on NO oxidation over platinum.

In presence of oxygen and NO, propene can be consumed by: (i) oxidation with oxygen, (ii) oxidation by NO_2 and (iii) selective catalytic reduction of NO (SCR). Oxidation by NO_2 or oxygen is indicated by the decrease of propene concentration, whereas SCR can be identified by simultaneous consumption of NO and propene. Surface nitrates species are also able to oxidize propene [34,35], which would release NO_x. Pt/Al_2O_3 catalysts are known to be active for SCR at low temperature and produce a significant amount of N_2O. The oxidation of NO to NO_2 and the subsequent reaction between NO_2 and propene is a mechanism put forward in several studies to explain the inhibition of NO oxidation by propene [23,33]. The concentration of propene and NO_x during a temperature ramp, centered at the propene ignition temperature, provides information to determine the pre-dominant reaction mechanism.

Propene oxidation was examined in Fig. 8 in the case of Pt/Al_2O_3 catalyst. The reaction started at ca. 170 °C. At the same time, reduction of NO by propene (SCR) occurred, which was evidenced by the consumption of NO_x. As suggested by the NO_x concentration drop, SCR rate increased with temperature up to ca. 265 °C. This temperature corresponds to the maximum SCR rate and to a propene conversion very close to 100%. NO_2 was detected in the outlet gas only after almost total propene conversion but NO_2 might have been formed by NO oxidation and subsequently used to directly oxidize C_3H_6 or consumed in the SCR reaction before it exited the catalyst.

As previously observed, propene and NO oxidation occur at lower temperature on bimetallic Pt–Pd catalysts, which suggests different light-off mechanisms for propene. In Fig. 9, it can be noticed that the propene concentration decrease was accompanied by a release of NO, which was compatible with a reaction between nitrate species and propene [34,35]. After this first step, the chain of reactions observed on Pt/Al_2O_3 took place. Reduction of NO by propene, C_3H_6 oxidation by oxygen and/or intermediate NO_2 and, after almost all propene has been consumed, NO oxidation

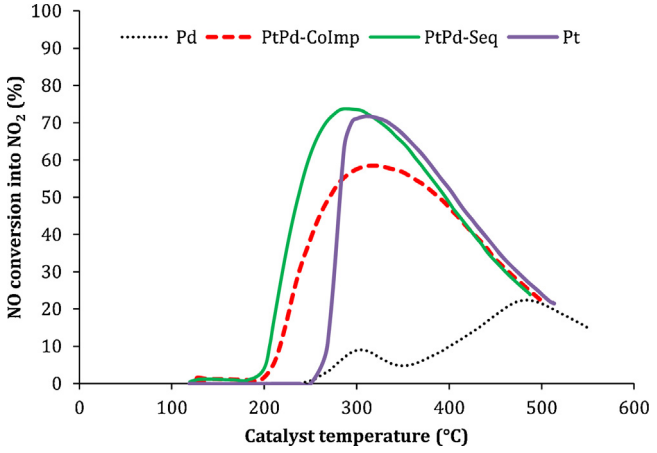

Fig. 7. NO conversion profile obtained during heating, in presence of 500 ppm C_3H_6. Comparison of monometallic (Pt, Pd) and bimetallic (Pt–Pd) catalysts.

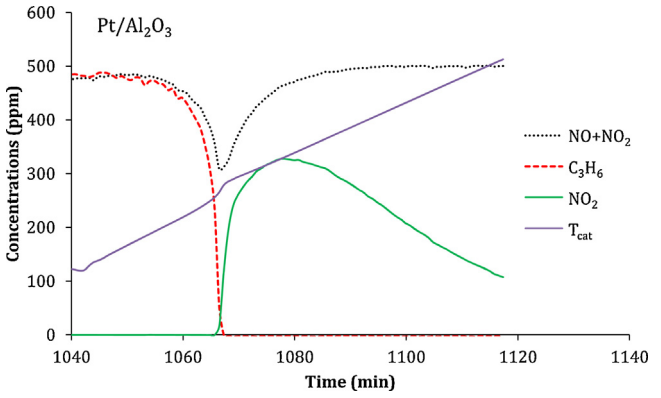

Fig. 8. The outlet concentration of propene, NO_2 and NO + NO_2 during heating to 500 °C for Pt/Al_2O_3. Gas flow composition: 500 ppm NO, 500 ppm C_3H_6, 8% O_2 balanced with Ar.

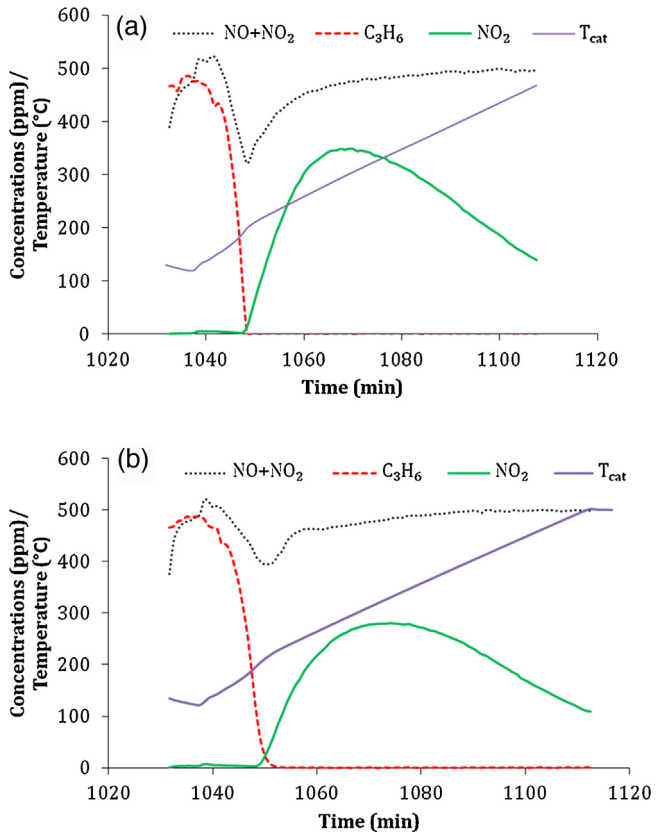

Fig. 9. The outlet concentration of propene, NO_2 and $NO + NO_2$ during heating to 500 °C and propene combustion ignition for Pt–Pd/Al_2O_3 (a) prepared by sequential impregnation and (b) prepared by co-impregnation. Gas flow composition: 500 ppm NO, 500 ppm C_3H_6, 8% O_2 balanced with Ar.

occurred. It seems that the inhibition of NO oxidation by propene was due to the blocking of sites by the hydrocarbon. Once propene started to be oxidized, vacant active sites were created, where other reactions consuming propene could proceed, leading to a subsequent sharp decrease of propene concentration. On Pt/Al_2O_3, SCR was identified as the trigger reaction of this chain mechanism, while on Pt-Pd catalysts, oxidation of propene by surface nitrates could be inferred to be the starting point. These two start-up mechanisms of propene oxidation operate at different temperature. The initial propene oxidation by nitrates occurs at lower temperature (125 °C) than the SCR on Pt/Al_2O_3 (175 °C). Thus, the presence of the reactive NO_x species adsorbed on the bimetallic catalysts, able to oxidize propene at low temperature, explains the better low temperature oxidation ability of the bimetallic Pt-Pd catalysts. It can be noted from Fig. 8 and 9 that on Pt/Al_2O_3, the amount of NO_x reduced by SCR was larger than on Pt–Pd (CoImp). At high enough temperature, all propene was consumed but NO oxidation was still affected by propene through SCR reaction, which consumed NO and competed with NO oxidation. Indeed, the NO_x concentration in Figs. 8 and 9 showed that SCR was occurring over a large temperature range after total propene conversion. This SCR temperature window was particularly broad on Pt/Al_2O_3 catalyst compared to PtPd (CoImp).

3.5. DRIFT study of NO and C_3H_6 adsorption

In order to identify the surface species formed on the studied catalysts, DRIFT measurements were conducted during exposure of the catalyst powder to $NO + O_2$ and $NO + O_2 + C_3H_6$ at 150 °C and 250 °C, which correspond to temperature before and after the propene light-off. Fig. 10 displays the absorption bands detected on Pt/Al_2O_3 and Pd/Al_2O_3. In absence of propene (Fig. 10, curves a and b), bands at 1235 and 1305 cm^{-1} were observed on both catalysts as well as a broad band in the 1500–1600 cm^{-1} region and a peak at 1616 cm^{-1}. They were assigned to nitrite (1235 cm^{-1}) [34] and nitrate (1305, 1500–1600, 1616 cm^{-1}) on alumina [36]. An additional unresolved band at 1400–1460 cm^{-1} was found on Pd/Al_2O_3. The co-adsorption of NO and propene in oxygen excess (Fig. 10, curves c and d) resulted in additional bands, attributed to carboxylate groups on alumina, at 1590, 1455, 1392 and 1370 cm^{-1}. The first two strong peaks were assigned to acetate [35] and the last two were assigned to formate [35–37]. At 150 °C on Pt/Al_2O_3, the nitrite peak at 1235 cm^{-1} was still present and the absorption due to nitrate at 1542 cm^{-1} was more intense than the absorption due to acetate at 1590 cm^{-1}. At 250 °C, only carboxylate bands remained on the Pt/Al_2O_3 spectra, indicating that propene replaced all nitrate species. On Pd/Al_2O_3, the nitrite band at 1235 cm^{-1} disappeared already at 150 °C and absorption due to carboxylate (1590 cm^{-1}) was more intense than the nitrate one in the 1500–1600 cm^{-1} region. However, at 250 °C, peaks related to nitrate species were still visible at 1653 and 1305 cm^{-1}. These results suggest that, at 150 °C, nitrate species have higher stability on Pt/Al_2O_3 while on Pd/Al_2O_3 carboxylate species resulting from propene adsorption were present in significant amount along nitrate species. At 250 °C, nitrates were totally replaced on Pt/Al_2O_3 surface while some nitrate species were still present on Pd/Al_2O_3 along with formates and acetates.

Fig. 11 shows the infrared spectra of bimetallic catalyst PtPd-CoImp and PtPd-Seq between 1100 and 1800 cm^{-1}. The features assigned to nitrate on alumina (1616, 1500–1600 and 1305 cm^{-1}) were also observed on bimetallic catalysts after exposure to $NO + O_2$ at 150 °C (Fig. 11, curve (a). The band assigned previously to nitrite (1235 cm^{-1}) was less pronounced at this temperature compared to nitrate (1305 cm^{-1}). At 250 °C (b), however, the bands at 1235 and 1305 cm^{-1} had similar intensity. The unresolved band found on Pd/Al_2O_3 at 1400–1460 cm^{-1} (Fig. 10 right) was observed on both PtPd-CoImp and PtPd-Seq at 150 °C only. In presence of propene, acetate (1590 and 1455 cm^{-1}) and formate (1392 and 1370 cm^{-1}) were formed on the surface. At 150 °C, nitrate and nitrites species were still present (strong band at 1305 cm^{-1} and shoulder at 1235 cm^{-1}). In parallel the strong band due to acetate appeared at 1590 cm^{-1}. On PtPd-CoImp like on Pt/Al_2O_3, the nitrate band at 1542 cm^{-1} was more intense than the acetate band at 1590 cm^{-1}. Another similarity between Pt/Al_2O_3 and PtPd-CoImp was the relatively low intensity of the peaks due to formates (1392 and 1370 cm^{-1}) at 150 °C. Similarly, on PtPd-Seq like on Pd/Al_2O_3, the absorption band at 1500–1600 cm^{-1} was dominated by the acetate contribution (1590 cm^{-1}) at 150 °C. The characteristics of Pd/Al_2O_3 are more marked on PtPd-Seq than on PtPd-CoImp which may indicate that more palladium was available on the surface of the particles in the catalyst prepared by sequential impregnation of platinum and then of palladium than on the sample

Table 3
Temperature of 50% (T_{50}) C_3H_6 conversion (in °C) measured during heating and cooling in presence of 500 ppm NO and 8% O_2.

Gas conditions	Pt		Pd		PtPd-Seq		PtPd-CoImp	
	Heating	Cooling	Heating	Cooling	Heating	Cooling	Heating	Cooling
500 ppm NO, 500 ppm C_3H_6, 8% O_2	244	240	201	208	175	176	177	171
500 ppm NO, 500 ppm C_3H_6, 8% O_2 + 5% H_2O	244	241	200	225	164	175	173	177

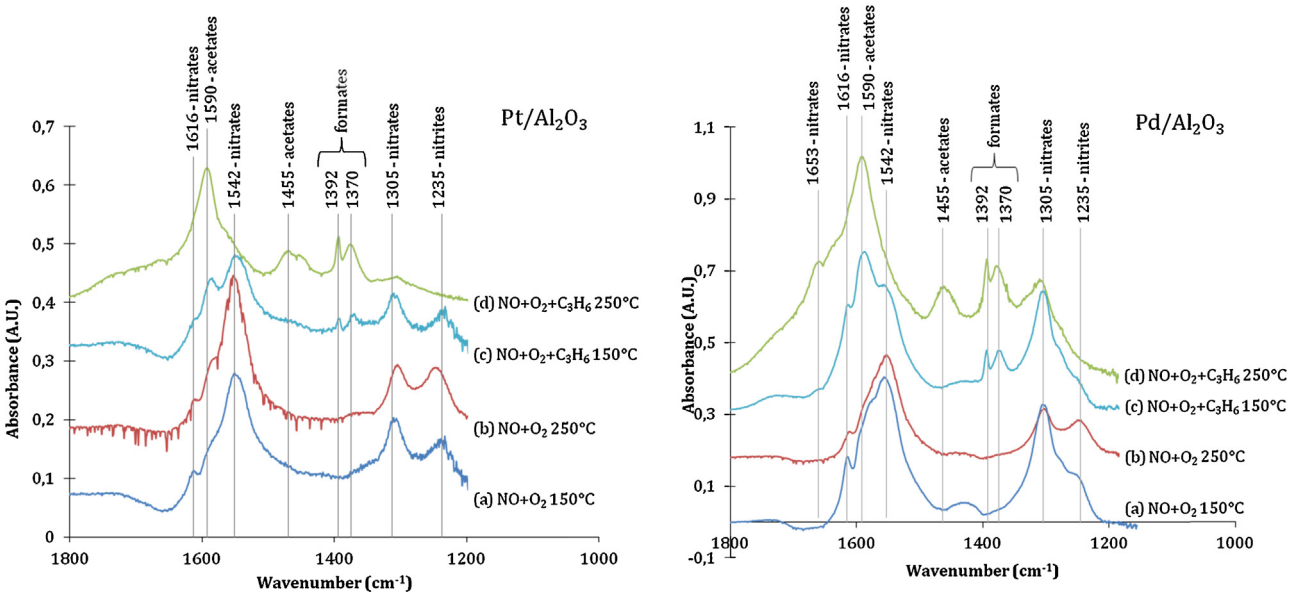

Fig. 10. Infrared absorption spectra in the region 1800–1100 cm^{-1} of Pt/Al_2O_3 (left) and Pd/Al_2O_3 (right) after 30 min exposure to (a) 1000 ppm NO + 8% O_2 at 150 °C, (b) 1000 ppm NO + 8% O_2 at 250 °C, (c) 1000 ppm NO + 1000 ppm C_3H_6 + 8% O_2 at 150 °C and (d) 1000 ppm NO + 1000 ppm C_3H_6 + 8% O_2 at 250 °C.

prepared by co-impregnation of the two metals. According to our adsorption experiments, the presence of palladium seems to facilitate the decomposition of propene to form acetate and formate at lower temperature. This result is in agreement with the activity results, which showed propene oxidation at lower temperature on bimetallic catalysts than on Pt/Al_2O_3. Since the NO oxidation started after almost full propene combustion, the presence of Pd indirectly enhanced the low temperature NO oxidation activity.

Fig. 12 presents the infrared absorption spectra of Pt/Al_2O_3 and Pd/Al_2O_3 exposed to 1000 ppm NO, 1000 ppmC_3H_6 and 8% O_2 in the 2000–3000 cm^{-1} range. Bands at 2900 cm^{-1}, 2300–2400 cm^{-1} and 2210–2260 cm^{-1} appeared on Pt/Al_2O_3 at 250 °C (a) but were absent at 150 °C (b). The band at 2900 cm^{-1} can be attributed to the stretching of C—H bonds of hydrocarbon fragments. The feature between 2300 and 2400 cm^{-1} is the characteristic signature of gas phase CO_2, which indicates propene oxidation. The absorption band at 2210–2260 cm^{-1} can be assigned to isocyanate species on alumina [36–39]. These bands were also observed on Pd/Al_2O_3 at 250 °C. In addition, a broad band at 2180 cm^{-1}, with a shoulder at 2135 cm^{-1} was noted on Pd/Al_2O_3 and assigned to cyanide species in agreement with literature identification [36,38]. Some authors assigned the band at 2180 cm^{-1} to the asymetric stretching vibration of NCO [40]. Thus this band was attributed to cyanide or isocyanate with different stability than the one identified at higher wavenumber (2210–2260 cm^{-1}). The presence of the hydrocarbon and the bands at 2180 cm^{-1} at 150 °C on Pd/Al_2O_3 demonstrated the interaction between propene surface species and nitrates on Pd-containing catalysts at low temperature. This evidence of surface reaction was absent on Pt/Al_2O_3 at 150 °C. Since isocyanate is thought to be an intermediate species in the NO_x reduction by propene [38], the presence of surface isocyanates (2210–2260 cm^{-1}) on Pt/Al_2O_3 agrees with the propene combustion mechanism inferred from the flow reactor experiments. On Pt/Al_2O_3 catalyst, propene combustion is initiated by the forma-

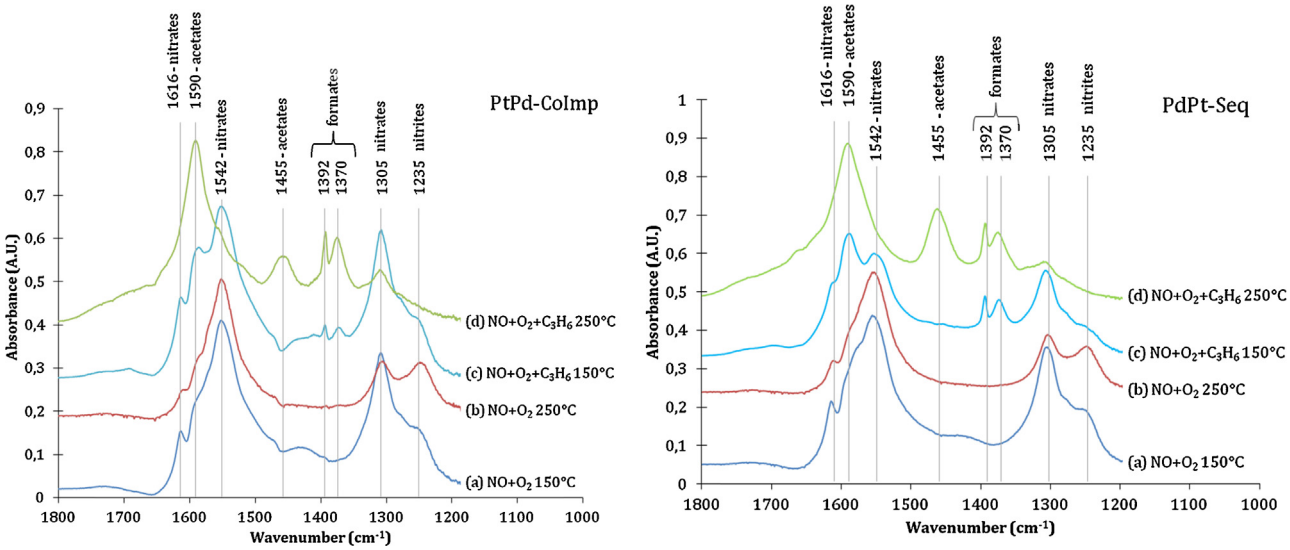

Fig. 11. Infrared absorption spectra in the region 1800–1100 cm^{-1} of PtPd-CoImp (left) and PtPd-Seq (right) after 30 min exposure to (a) 1000 ppm NO + 8% O_2 at 150 °C, (b) 1000 ppm NO + 8% O_2 at 250 °C, (c) 1000 ppm NO + 1000 ppm C_3H_6 + 8% O_2 at 150 °C and (d) 1000 ppm NO + 1000 ppm C_3H_6 + 8% O_2 at 250 °C.

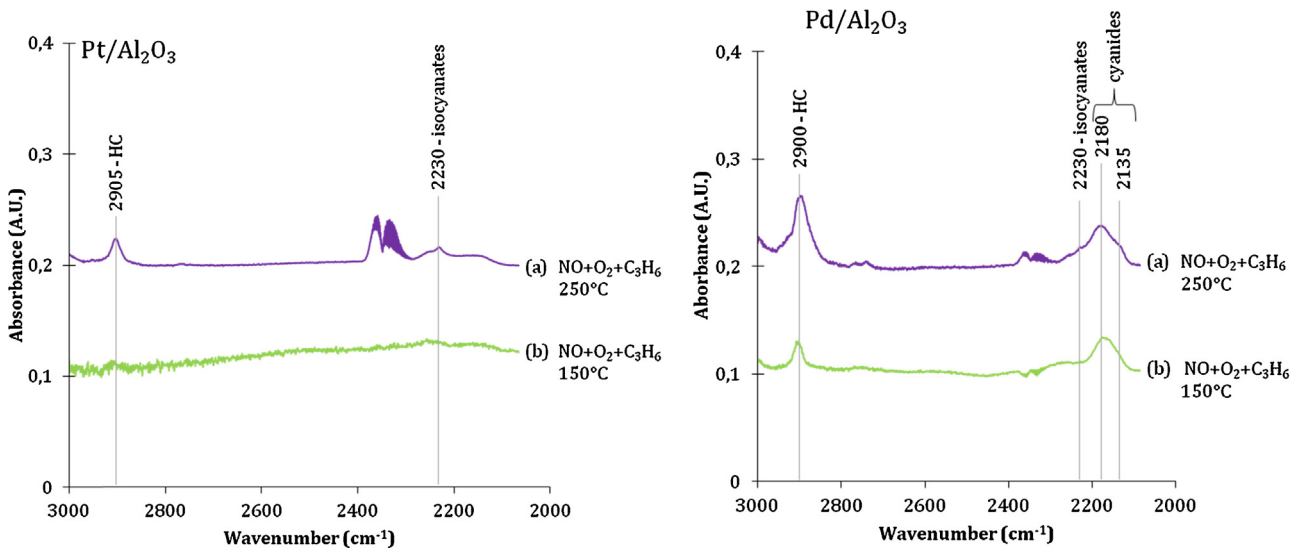

Fig. 12. Infrared absorption spectra in the region 3000–2000 cm^{-1} of Pt/Al_2O_3 (left) and Pd/Al_2O_3 (right) after 30 min exposure 1000 ppm NO + 1000 ppm C_3H_6 + 8% O_2 at (a) 150 °C and (b) 250 °C.

tion and reduction of isocyanates according to the NO_x reduction by propene reaction. Unlike on Pt/Al_2O_3, species absorbing at 2130–2180 cm^{-1}, assigned to cyanide [36,38], were predominantly formed on Pd/Al_2O_3 surface, which suggests a different propene utilization on this catalyst and correlates the flow reactor experiments. On palladium-containing catalysts, reaction of adsorbed propene with nitrates is the initial step suggested by the flow reactor experiments. The formation of cyanide (or possibly isocyanate with different stability than on Pt/Al_2O_3) at lower temperature than the propene-SCR of NO_x showed also the good ability of propene and nitrates to interact on these catalysts.

Fig. 13 shows the spectra acquired on the bimetallic samples in the range 2000–3000 cm^{-1} after exposure to 1000 ppm NO, 1000 ppm C_3H_6 and 8% O_2 for 30 min. The bands at 2900, 2250 and 2180 cm^{-1} previously identified as hydrocarbon fragments, isocyanate and cyanide respectively were observed on both bimetallic catalysts at 150 °C and 250 °C. However on bimetallic samples, like on Pd/Al_2O_3, the absorption band at 2130–2180 cm^{-1} was more intense than the isocyanate band. It can be noticed that at 150 °C less species were formed on PtPd-CoImp in the 2000–3000 cm^{-1} region, which was characteristic of Pt/Al_2O_3. In contrary, PtPd-Seq and Pd/Al_2O_3 presented both significant surface hydrocarbons and cyanide (or isocyanate) at 150 °C, which confirms the greater influence of palladium on the catalyst prepared by sequential impregnation. This result correlates well the flow reactor experiments, which showed a greater activity for PtPd-Seq than PtPd-CoImp in presence of propene (Fig. 7).

3.8. *Effect of palladium*

The addition of palladium in the formulation of DOCs contributes to a greater thermal stability [6–10]. Our results showed that stable and reproducible performance was reached more rapidly by bi-metallic catalysts than by Pt/Al_2O_3. The resistance to strong platinum oxide formation was enhanced by the presence of Pd. Bi-metallic catalysts demonstrated improved ability to handle a gas mixture that contained both NO and C_3H_6, which are known to inhibit each other's oxidation on Pt/Al_2O_3. The total inhibition of NO oxidation due to propene on Pt/Al_2O_3 was illustrated in Fig. 4, where it can be seen that, during a temperature ramping, nitric

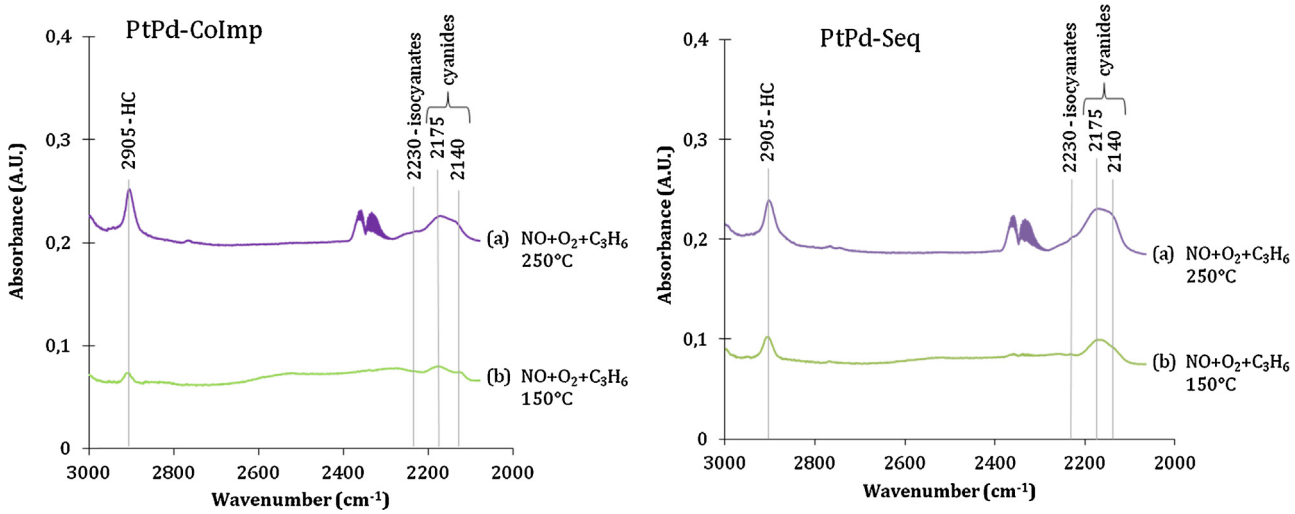

Fig. 13. Infrared absorption spectra in the region 3000–2000 cm^{-1} of PtPd-CoImp (left) and PtPd-Seq (right) after 30 min exposure 1000 ppm NO + 1000 ppm C_3H_6 + 8% O_2 at (a) 150 °C and (b) 250 °C.

oxide conversion remained null at low temperature until almost all propene was oxidized. The presence of palladium decreased tremendously the C_3H_6 oxidation light-off temperature in presence of NO, thus limiting the propene inhibiting effect. Higher catalytic activity for hydrocarbon combustion by addition of Pd was also observed by Haneda et al. [9] on Pt/Al_2O_3.

Propene combustion needs to be initiated in order to increase the surface temperature and to decrease the propene coverage. The release of NO_x concomitant to the propene conversion on Pt–Pd catalysts (Fig. 9) suggests the oxidation of propene by nitrate surface species as initiating step. The simultaneous conversion of NO_x and propene on Pt/Al_2O_3 (Fig. 8) suggests that NO_x SCR by propene as starting step on this catalyst. The DRIFT study evidenced the decomposition of propene and the formation of species involving both propene and NO, such as cyanide and isocyanate, on the surface of Pd-containing catalysts at 150 °C (see Figs. 12 and 13). These species were not observed on Pt/Al_2O_3 at such low temperature, indicating greater reactivity of propene at low temperature on Pd-containing catalysts. These results agree well with our flow reactor activity tests. Further, we have observed that the presence of palladium promotes the propene combustion, while high NO conversion requires platinum, as indicated by the poor NO oxidation performance of Pd/Al_2O_3.

4. Conclusions

Diesel oxidation catalysts containing palladium and platinum, alone or in combination, were studied in flow reactor to evaluate their NO oxidation ability in various conditions. In particular, the effect of water and propene on the activity was evaluated. The stability of the catalyst has shown to be an important parameter as the repetition of activity test led to an enhancement of the catalytic performance. The effect of palladium addition to Pt/Al_2O_3 was to reach reproducible activity more rapidly than Pt/Al_2O_3. The presence of water has been identified as one accelerating factor in the stabilization process of bi-metallic catalysts.

The presence of water yielded a global decrease of NO conversion on all catalysts, while propene showed a strong inhibiting effect at low temperature, i.e., lower than the propene combustion light-off. Due to the addition of palladium that conferred lower propene light-off temperature, the bimetallic catalysts stood out as the most active at low temperature in presence of propene. The infrared spectra indicated that on Pd-containing catalysts, propene could decompose and react with surface nitrates species already at 150 °C whereas this was not observed on Pt/Al_2O_3 at such low temperature. In addition, NO_x release was observed at the beginning of propene conversion on bimetallic catalysts, which agrees with the oxidation of propene with surface nitrate as the starting reaction of propene combustion. On Pt/Al_2O_3, NO_x reduction by propene, which occurred at higher temperature, was identified as the reaction initiating the propene combustion.

The preparation method of the Pt-Pd catalysts had a great influence on the catalytic properties and activity. The sequential impregnation of the metal, starting with Pt, yielded higher performance than Pt/Al_2O_3 and pronounced similarities as Pd/Al_2O_3 in adsorption properties, such as decomposition of propene and formation of cyanide surface species at 150 °C. However, this catalyst, like Pt/Al_2O_3, was able to form strong platinum oxide after aging which improves its NO oxidation ability. The catalyst prepared by co-impregnation of both metals showed similar or slightly lower activity than Pt/Al_2O_3 depending on the conditions. To conclude the bimetallic catalyst prepared by sequential impregnation exhibited the best performance of all studied catalysts.

Acknowledgements

The work is financially supported by Swedish Foundation for Strategic Research (F06-0006) and the Swedish Research Council) (621-2011-4860) and was performed at the Competence Center for Catalysis, which is hosted by Chalmers University of Technology and financially supported by the Swedish Energy Agency and the member companies AB Volvo, ECAPS AB, Haldor Topsøe A/S, Scania CV AB, Volvo Car Corporation AB and Wärtsilä Finland Oy.

References

[1] X. Auvray, T. Pingel, E. Olsson, L. Olsson, Appl. Catal. B: Environ. 129 (2013) 517–527.
[2] S.K. Matam, E.V. Kondratenko, M.H. Aguirre, P. Hug, D. Rentsch, A. Winkler, A. Weidenkaff, D. Ferri, Appl. Catal. B: Environ. 129 (2013) 214–224.
[3] Y.F. Chu, E. Ruckenstein, J. Catal. 55 (1978) 281–298.
[4] P.C. Flynn, S.E. Wank, J. Catal. 37 (1975) 432–448.
[5] M. Kaneeda, H. Iizuka, T. Hiratsuka, N. Shinotsuka, M. Arai, Appl. Catal. B: Environ. 90 (2009) 564–569.
[6] G.W. Graham, H.W. Jen, O. Ezekoye, R.J. Kudla, W. Chun, X.Q. Pan, R.W. McCabe, Catal. Lett. 116 (2007) 1–8.
[7] M. Chen, L.D. Schmidt, J. Catal. 56 (1979) 198–218.
[8] A. Morlang, U. Neuhausen, K. Klementiev, F. Schutze, G. Miehe, H. Fuess, E. Lox, Appl. Catal. B: Environ. 60 (2005) 191–199.
[9] M. Haneda, K. Suzuki, M. Sasaki, H. Hamada, M. Ozawa, Appl. Catal. A: Gen. 475 (2014) 109–115.
[10] O.K. Ezekoye, A.R. Drews, H.W. Jen, R.J. Kudla, R.W. McCabe, M. Sharma, J.Y. Lowe, L.F. Allard, G.W. Graham, X.Q. Pan, J. Catal. 280 (2011) 125–136.
[11] M. Kröcher, M. Widmer, Ind. Eng. Chem. Res. 48 (22) (2009) 9847–9857.
[12] X.P. Auvray, L. Olsson, Ind. Eng. Chem. Res. 52 (2013) 14556–14566.
[13] H.C. Yao, H.K. Stepien, H.S. Gandhi, J. Catal. 7 (1) (1981) 231–236.
[14] H.S. Gandhi, M. Shelef, Appl. Catal. 77 (1991) 175–186.
[15] M. Kärkkäinen, M. Honkanen, V. Viitanen, T. Kolli, A. Valtanen, M. Huuhtanen, K. Kallinen, M. Vippola, T. Lepistö, J. Lahtinen, R.L. Keiski, Top. Catal. 56 (2013) 672–678.
[16] T. Kolli, M. Huuhtanen, M. Vippola, K. Kallinen, T. Kinnunen, T. Lepistö, J. Lahtinen, R.L. Keiski, Catal. Today 154 (2010) 303.
[17] K. Hauff, U. Tuttlies, G. Eigenberger, U. Nieken, Appl. Catal. B: Environ. 123–124 (2012) 107–116.
[18] A. Boubnov, S. Dahl, E. Johnson, A.P. Molina, S.B. Simonsen, F.M. Cano, S. Helveg, L.J. Lemus-Yegres, J.-D. Grunwaldt, Appl. Catal. B: Environ. 126 (2012) 315–325.
[19] W. Hauptmann, M. Votsmeier, J. Gieshoff, A. Drochner, H. Vogel, Appl.Catal. B: Environ. 93 (2009) 22–29.
[20] K. Hauff, U. Tuttlies, G. Eigenberger, U. Nieken, Appl. Catal. B: Environ. 100 (2010) 10–18.
[21] L. Olsson, M. Abul-Milh, H. Karlsson, E. Jobson, P. Thormählen, A. Hinz, Top. Catal. 30–31 (2004) 85–90.
[22] H. Oh, J. Luo, W.S. Epling, Catal. Lett. 141 (2011) 1746–1751.
[23] M. Al-Harbi, R. Hayes, M. Votsmeier, W.S. Epling, Can. J. Chem. Eng. 90 (2012) 1527–1538.
[24] P. Denton, A. Giroir-Fendler, H. Praliaud, M. Primet, J. Catal. 189 (2000) 410–420.
[25] S.S. Mulla, N. Chen, L. Cumaranatunge, G.E. Blau, D.Y. Zemlyanov, W.N. Delgass, W.S. Epling, F.H. Ribeiro, J. Catal. 241 (2006) 389–399.
[26] L. Olsson, E. Fridell, J. Catal. 210 (2002) 340–353.
[27] E. Xue, K. Seshan, J.R.H. Ross, Appl. Catal. B: Environ. 11 (1996) 65–79.
[28] F. Tao, M.E. Grass, Y. Zhang, D.R. Butcher, J.R. Renzas, Z. Liu, J.Y. Chung, B.S. Mun, M. Salmeron, G.A. Somorjai, Science 322 (2008).
[29] L. Fiermans, R. De Gryse, G. De Doncker, P.A. Jacobs, J.A. Martens, J. Catal. 193 (2000) 108–114.
[30] M. Harada, K. Asakura, Y. Ueki, N. Toshima, J. Phys. Chem. 96 (1992) 9730–9738.
[31] T. Fujikawa, K. Tsuji, H. Mizukuchi, H. Godo, K. Idei, K. Usui, Catal. Lett. 63 (1999) 27–33.
[32] A.V. Kalinkin, A.M. Sorokin, M. Yu. Smirnov, V.I. Bukhtiyarov, Kinet. Catal. 55 (3) (2014) 354–360.
[33] K. Irani, W.S. Epling, R. Blint, Appl. Catal. B: Environ. 92 (2009) 422–428.
[34] S. Chansai, R. Burch, C. Hardacre, H. Oh, W.S. Epling, Catal. Sci. Technol. 3 (2013) 2349–2356.
[35] K. Shimizu, H. Kawabata, A. Satsuma, T. Hattori, J. Phys. Chem. B 103 (1999) 5240–5245.
[36] D.K. Captain, M.D. Amiridis, J. Catal. 184 (1999) 377–389.
[37] M. Huuhtanen, T. Kolli, T. Maunula, R.L. Keiski, Catal. Today 75 (2002) 379–384.
[38] N. Bion, J. Saussey, M. Haneda, M. Daturi, J. Catal. 217 (2003) 47–58.
[39] F. Solymosi, T. Bánsági, J. Catal. 202 (2001) 205–206.
[40] F. Solymosi, J. Raskó, Appl. Catal. 10 (1984) 19–25.